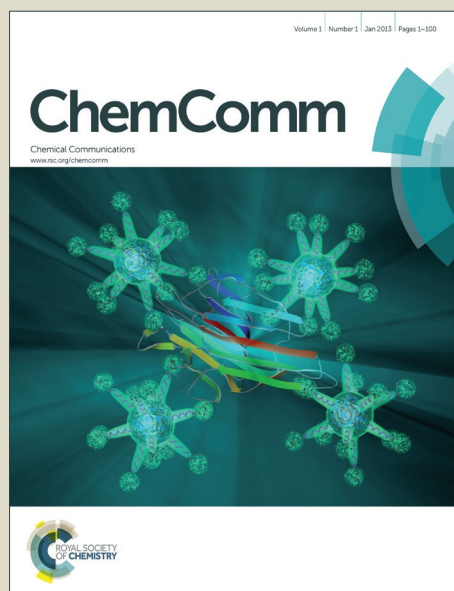


ChemComm

Accepted Manuscript



This is an *Accepted Manuscript*, which has been through the Royal Society of Chemistry peer review process and has been accepted for publication.

Accepted Manuscripts are published online shortly after acceptance, before technical editing, formatting and proof reading. Using this free service, authors can make their results available to the community, in citable form, before we publish the edited article. We will replace this *Accepted Manuscript* with the edited and formatted *Advance Article* as soon as it is available.

You can find more information about *Accepted Manuscripts* in the [Information for Authors](#).

Please note that technical editing may introduce minor changes to the text and/or graphics, which may alter content. The journal's standard [Terms & Conditions](#) and the [Ethical guidelines](#) still apply. In no event shall the Royal Society of Chemistry be held responsible for any errors or omissions in this *Accepted Manuscript* or any consequences arising from the use of any information it contains.



Chemical Communications

COMMUNICATION

A novel dimethylformamide (DMF) free bar-cast method to deposit organolead perovskite thin films with improved stability

Received 00th January 20xx,
Accepted 00th January 20xx

DOI: 10.1039/x0xx00000x

www.rsc.org/

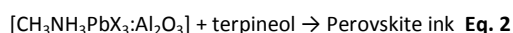
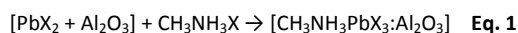
Eurig W. Jones^a, Peter J. Holliman^{a*}, Arthur Connell^a, Matthew L. Davies^b, Jennifer Baker^b, Robert J. Hobbs^a, Sanjay Ghosh^a, Leo Furnell^a, Rosie Anthony^a and Cameron Pleydell-Pearce^b

We report a solvent-free approach to synthesizing organolead perovskites by using solid state reactions to coat perovskite crystals onto Al₂O₃ or TiO₂ nanoparticles followed by addition of terpineol affording perovskite inks. We have bar cast these inks to produce photoactive perovskite thin films which are significantly more stable to humidity than solution-processed films. This new method also avoids the use of toxic DMF solvent.

Since the initial reports of organolead halide perovskite solar cells^{1,2}, device efficiencies have risen rapidly towards 20%³. It has also been demonstrated that such perovskites work efficiently in a variety of PV device architectures⁴ including planar TiO₂ charge collection layers⁵ and mesoporous TiO₂ as well as in batteries^{6a} and sensors^{6b}. Electrically-insulating Al₂O₃ scaffolds¹ and even hole transporter-free perovskite devices⁷ have been reported, demonstrating that the perovskite absorber layer can efficiently sustain charge transport. This is important because key limiting factors for perovskite solar cells are the surface coverage and crystallisation steps which occur at the perovskite-metal oxide interface during device manufacture. As a result, perovskite device manufacturing is the subject of much interest. A current limitation for one-step, solution processed perovskites is infiltration into the mesoporous scaffold, which can be improved by sequential deposition⁸, affording superior coverage and avoiding the need for a perovskite capping layer. However, concerns remain over the solvents used for solution processed perovskites⁹ and the stability of the resulting materials to temperature and/or moisture^{10, 11}. As such, recent reports suggest optimum fabrication conditions such as %RH<1%¹⁰ which complicates scale up.

To date, the choice of perovskite processing solvent has been limited to dimethylformamide (DMF)¹, dimethylsulfoxide (DMSO)¹² or γ -butyrolactone (GBL)² given the need to dissolve the PbX₂ precursor (X = Cl, Br, I). By comparison, methyl ammonium halides are readily soluble in most solvents including water. In this paper,

we report that a 1:1 ratio of PbX₂ and CH₃NH₃X react readily together with quantitative yield in solvent-free, solid state reactions by grinding/milling (ESI Fig. 1). We have also studied the addition of metal oxide nanoparticles (Al₂O₃ or TiO₂) as common scaffold materials for perovskite solar cells during or after the solid state perovskite reaction. After perovskite has formed on the metal oxide surface, to produce a printable ink, we have ground the particles in terpineol as a suspending media rather than a solvent. Perovskite crystals have previously been suspended in DMF¹² but here terpineol has been chosen because it has low toxicity and is widely used in printing media. It also possesses a high boiling point (219 °C), which is similar to DMSO (189 °C) which has been reported to stabilise solvent–PbI₂ complexes and inhibit PbI₂ crystallization¹³. This also avoids the DMF volatilisiation (b.p. 153 °C) during spin coating, which increases perovskite crystal dislocations. Higher boiling solvents also encourage slower perovskite crystal growth during annealing. The resultant inks can then be doctor bladed or bar cast. We have studied the influence of metal oxide loading and found that, for Al₂O₃, a loading of >10% Al₂O₃ is required to cast a uniform layer, presumably because Al₂O₃ acts as a plasticizer. This is more than the 5% Al₂O₃ reported by Carnie *et al.*¹⁴ for their DMF/perovskite/Al₂O₃ nanoparticle precursor in their spin coating based study. The difference is that the perovskite particles are pre-formed on the Al₂O₃ particle surfaces in our inks and no DMF is present unlike previous reports of bar-cast perovskites¹⁵. Visual inspection also suggests that the resulting colloidal inks are stable for >3 months. An additional advantage of developing inks for meso-scopic perovskite solar cells using a passive Al₂O₃ scaffold is their low-temperature processability. Thus, our inks can be deposited under ambient conditions and heated at 110 °C because high temperature processing is not required to ensure inter-particle “necking” to carry electrical charge as is the case for TiO₂ photo-electrodes¹⁶. This is in line with previous reports for Al₂O₃ where heat processing is shown to be complete at 150 °C¹⁷ and 110 °C¹⁴. The perovskite ink formation is described in Equations 1 and 2.



^a School of Chemistry, Bangor University, Bangor, Gwynedd LL57 2UW UK
^b SPECIFIC, Swansea University, Swansea, SA1 8EN U.K.

Electronic Supplementary Information (ESI) available: [details of any supplementary information available should be included here]. See DOI: 10.1039/x0xx00000x

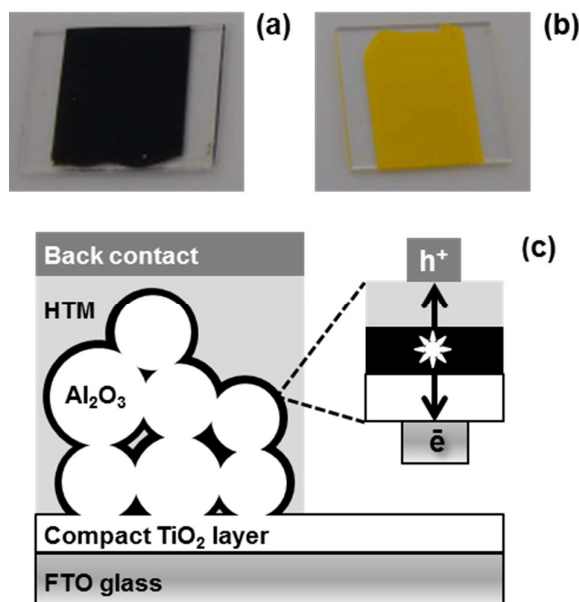


Fig. 1 (a) semi-perovskite, (b) perovskite intermediate and (c) schematic of perovskite device architecture

For film deposition, a compact 80nm TiO₂ layer (Solaronix BL) was spin coated (3500rpm, 60s) onto TEC15 glass (15Ωsq⁻¹, NSG) and heated (550°C for 1h). Perovskite inks were deposited onto these substrates either by spin coating, doctor blading or bar casting to produce films ranging from 400 nm to ca. 10 μm in thickness. In addition, to drastically increasing the atom efficiency of the perovskite manufacturing process, the stoichiometric nature of these solid state reactions is key to improving the compositional control over the materials produced. Thus, in Snaith *et al.* original report of perovskite devices¹, a 3:1 ratio of CH₃NH₃I:PbCl₂ was used along with spin coating to control layer thickness. However, the I:Cl ratio of the resultant CH₃NH₃PbI₂Cl was reported as 2:1. Effectively, this means that an excess of CH₃NH₃I is required to convert all the PbCl₂ into perovskite. Whilst CH₃NH₃X waste is less of an issue at the laboratory scale, it is not viable for a scaled process because it multiplies raw material costs and environmental impact which has been reported to be greater for CH₃NH₃I than for PbX₂¹⁸. By comparison, in the solid state reactions, CH₃NH₃X and PbX₂ can be reacted together in the desired ratio and this ratio is carried through into the resulting perovskite material. A further advantage of solid state reactions is much greater control of trace components (e.g. Cl⁻) which is known to be key to device performance¹⁹.

To prepare organolead perovskites on Al₂O₃, PbX₂ (X = Cl, Br, I) and Al₂O₃ nanoparticles (mean size 13 nm) are ground together until there is no further colour change. After adding the desired CH₃NH₃X to this the mixture is ground together again. Conversion to a perovskite phase varies depending on the halides used. For CH₃NH₃PbI_{3-x}Cl_x, an intermediate non-perovskite yellow phase is obtained (Fig. 1b) which only turns black and converts to perovskite after heating at 120 °C for 50min (*i.e.* standard solution processing

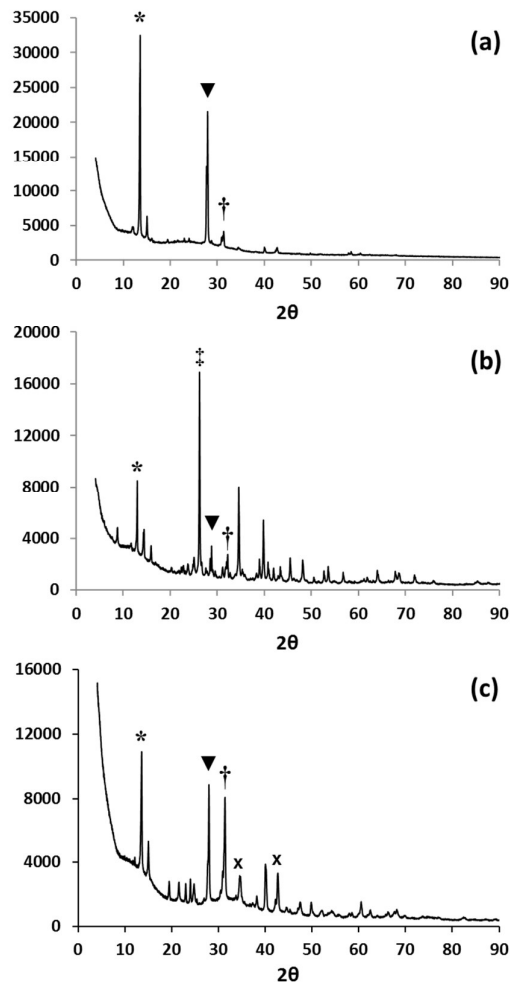


Fig. 2 XRD data of CH₃NH₃PbI₃ films manufactured by (a) solution processing, (b) solid state reaction using TiO₂ and (c) deposited on glass from a perovskite ink. * (110), ▼ (220), † (310) of perovskite phase, × (Al₂O₃), ‡ (101) TiO₂ diffraction lines.

conditions). A similar intermediate perovskite complex, has been previously reported by Wu *et al.*¹³. By comparison, the CH₃NH₃PbI₃ ink turns black purely by mechanical mixing and before heating at 120 °C (Fig. 1a). We have defined the pre-heated tri-iodide as “semi-perovskite” ink as the XRD data confirm significant amounts of unconverted PbI₂ are still present, which then decrease after heating. Finally, CH₃NH₃PbBr₃ turns orange on grinding which fully converts and increases in crystallinity on heating (ESI Fig. 3). Upon the addition of terpeneol, each reaction continues to completion and we believe the terpeneol assists in a wet grinding process whereby the size of the PbX₂ and CH₃NH₃X crystals are further reduced and these particles are more intimately mixed enabling intercalation of CH₃NH₃X into the lead halide lattice to form crystalline perovskite.

X-ray powder diffraction data show that the solid state reaction between CH₃NH₃I and PbI₂ produces predominantly the CH₃NH₃PbI₃ phase with only low intensity peaks observed for PbI₂ (Fig. 2b). Unconverted PbI₂ has been reported previously in the two-step

solution processing method, even when the substrate is heated to 60°C, to constrain lateral crystal growth²⁰. The PbI₂ peaks observed in our work (ground samples) more closely resemble data observed for samples deposited on optimally pre-heated (50°C) substrates, which is typically done to assist small particle formation and improve coverage¹³. After grinding in terpineol (Fig. 2c), the (110) peak for the perovskite phase increases in relative intensity, confirming that the solid state reaction continues on further grinding in the solvent. Data from line broadening suggest that the average crystal/domain size is *ca.* 100 nm which is similar to that typically observed purely for one-step solution processing methods rather than the larger 500nm particle sizes observed using the two-step method¹⁷. In addition for both ground samples, there is less evidence of preferred orientation (Fig. 2b-c) compared to solution deposited material (Fig. 2a). This is to be expected as the solution deposited samples nucleate and grow directly onto a flat substrate which is heated from below making perpendicular crystal growth much more likely. By comparison, the ground samples nucleate and crystallise onto randomly oriented metal oxide particles so the orientation of their crystal growth will also be randomised.

Photoluminescence (PL) of perovskite films is strongly linked to device efficiency²¹ and so PL microscopy and *in situ* spectroscopy of perovskite:metal oxide films was carried out to evaluate surface coverage and electron shuttling. The data show that films of doctor bladed CH₃NH₃PbI_{3-x}Cl_x, bar cast CH₃NH₃PbI_{3-x}Cl_x and CH₃NH₃PbBr₃ are all emissive, which suggests they should all be photo-active in PV devices (Fig. 3a-c). As expected, the thicker 7µm doctor bladed CH₃NH₃PbI_{3-x}Cl_x film (Fig. 3a, f) shows PL intensity which is much greater than that of the equivalent 400 nm bar cast film (Fig. 3b, f). Interestingly, the intensity of the doctor bladed film is comparable to the solution processed image (Fig. 3e, f). In terms of coverage, two issues need consideration. Firstly, there is the coverage of the mesoporous Al₂O₃ film on the substrate and secondly there is the coverage of the perovskite layer on the Al₂O₃ surface. For the doctor bladed film, the perovskite coverage on the Al₂O₃ surface appears to be consistent whilst the mesoporous Al₂O₃ film is much less even. However, there do not appear to be any pin holes in this film which would cause short circuiting in PV devices made from this material. By comparison, the coverage of the perovskite on the Al₂O₃ surface in the bar coated film appears less complete although the mesoporous Al₂O₃ film itself still appears to be complete. For the analogous bar coated CH₃NH₃PbBr₃ sample, greater PL intensity is observed than for the CH₃NH₃PbI_{3-x}Cl_x sample although at λ *ca.* 540nm reflecting the larger band gap for the tribromide perovskite. Here, the perovskite coverage on Al₂O₃ seems fairly complete although some areas seem brighter than others suggesting variable particle sizes of perovskite crystals have been deposited (Fig. 3c). To further study scaffold coverage, a TiO₂-based CH₃NH₃PbI₃ paste was bar coated onto a glass substrate. The maximum PL intensity for this sample is *ca.* 600cps compared to *ca.* 12000cps for the doctor bladed and *ca.* 6000cps bar coated CH₃NH₃PbI_{3-x}Cl_x films. Firstly, this suggests that the perovskite films formed can effectively inject into an electrically-conducting scaffold whilst the PL mapping (Fig. 3d) of TiO₂-based perovskite ink shows areas of low PL intensity across the film surface. As the films are not under load, we expect emission to be faster than injection so the

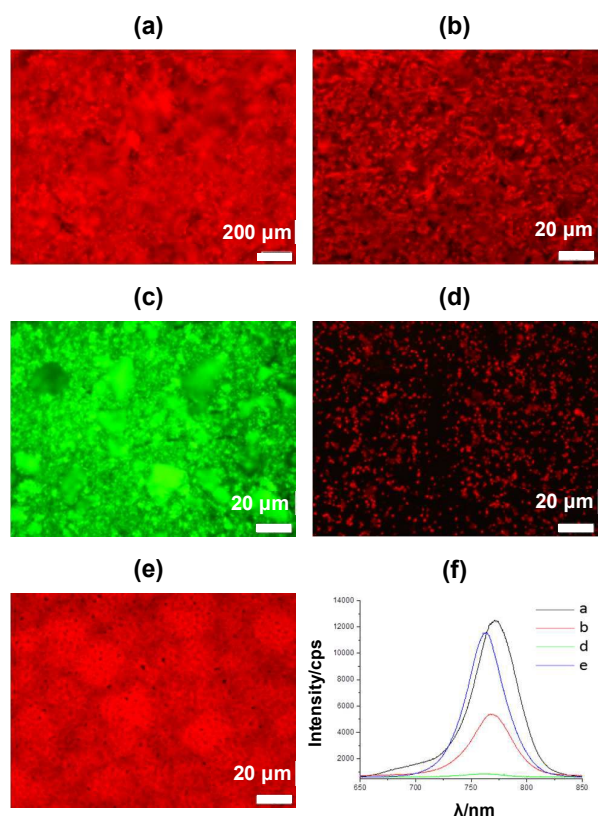


Fig. 3 Photoluminescence images of films of (a) 7µm, 2-step, doctor bladed CH₃NH₃PbI_{3-x}Cl_x, (b) 4µm wet thickness, bar cast sequential CH₃NH₃PbI_{3-x}Cl_x, (c) 4µm wet thickness, bar cast CH₃NH₃PbBr₃, (d) 4µm wet thickness, bar cast, one step TiO₂-CH₃NH₃PbI₃, (e) spun coated solution processed CH₃NH₃PbI_{3-x}Cl_x and (f) intensity vs. λ for selected PL image.

low emission for this film may reflect poor coverage or lower stability of the CH₃NH₃PbI₃ on TiO₂. By comparison, the more uniform emission across the perovskite:Al₂O₃ films confirms better coverage and perovskite stability and could also suggest lower losses at grain boundaries or crystal interfaces where emission might be quenched. Ultimately, assuming that more emission relates to more potential charge extraction in a PV device under load and given the need for PV devices to possess lifetimes of many years this suggests Al₂O₃ scaffolds should be preferable to TiO₂. Furthermore, perovskites which have been solution processed onto metal oxide scaffolds exhibit slightly blue-shifted emission (760 nm vs 750 nm) as a result of confined growth within mesoporous films^{22,23}. Fig. 3f shows that the PL peaks of the ink-based films are similarly blue shifted compared to the solution processed film. This suggests that the perovskite crystals from perovskite inks are similar in size to those grown inside scaffolds, using standard solution processed methods (i.e. typically <100 nm). Perovskite film morphology has also been investigated by SEM (ESI Figs. 5-8) which shows the best perovskite coverage for CH₃NH₃PbBr₃ ink in line with the higher intensity PL data for this film.

The lifetime of the perovskite films has also been studied (Fig. 4). The data show that Al₂O₃-based films exhibit significantly better

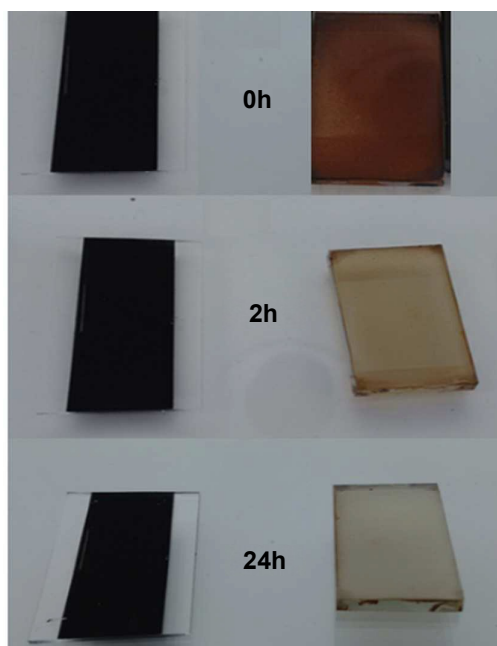


Fig. 4 (Left) bar-cast $\text{CH}_3\text{NH}_3\text{PbI}_3:\text{Al}_2\text{O}_3$ perovskite ink and (right) spin coated, solution processed $\text{CH}_3\text{NH}_3\text{PbI}_3$ films vs time

resistance to atmospheric exposure (air, humidity, light) than solution processed films. We have observed that the first stage of humidity-driven perovskite degradation involves phase separation into PbX_2 and $\text{CH}_3\text{NH}_3\text{X}$ but that both materials remain on the surface. Hence, in the early stages of degradation, the process can be reversed by heating at 100°C . However, this reversibility is only possible when the PbX_2 and $\text{CH}_3\text{NH}_3\text{X}$ are proximally located on the surface. As further phase separation occurs with time, this process becomes irreversible by heating. However, it can be reversed by drying, grinding and heating to re-mix the $\text{PbX}_2 + \text{CH}_3\text{NH}_3\text{X}$. Here, we believe that the stabilising influence of the Al_2O_3 is to slow the rate of phase separation and, in doing so, effectively to shift the equilibrium ($\text{PbX}_2 + \text{CH}_3\text{NH}_3\text{X} \leftrightarrow \text{CH}_3\text{NH}_3\text{PbX}_3$) towards perovskite. Interestingly, Al_2O_3 capping layers on the perovskite absorber layer have also been reported as moisture barriers¹⁰. TGA data (ESI Fig. 11, 12) suggest that some terpineol may remain after heating but that this reduces with increasing temperature and/or time. If terpineol acts as a solvent of crystallization it should slow H_2O ingress but residual solvent is not expected to limit PV efficiency as it has been reported that small amounts of inert media (e.g. PEG²⁴) do not limit device performance. However, removing all terpineol does not reduce film lifetime (ESI Fig. 12) suggesting surface perovskite: Al_2O_3 interactions may enhance film stability.

In summary, we have demonstrated that photo-active, organolead perovskites can be prepared by solid state reactions onto Al_2O_3 scaffolds producing materials with enhanced stability. Whilst this resolves key processing limitations by negating the need for toxic or hygroscopic solvents such as DMF, GBL or DMSO⁹, this approach also makes the synthesis of other (e.g. lead-free) organometallic perovskites much simpler as it avoids complex solvent engineering issues²⁵ or complex solvent-solvent extraction techniques²⁶. In addition, using solid state reactions

means that all the raw materials end up in the product which makes it easier to add trace components. Also the printing of pre-made perovskite inks is easily scalable whilst solution-based spin coating is not and the vast majority of precursor solutions are spun away making compositional control very difficult.

References

- M.M. Lee, J. Teuscher, T. Miyasaka, T.N. Murakami, H.J. Snaith, *Science*, 2012, **338**, 643.
- L. Etgar, P. Gao, Z. Xue, Q. Peng, A.K. Chandriran, B. Liu, M.K. Nazeeruddin, M. Grätzel, *J. Am. Chem. Soc.*, 2012, **134**, 17396.
- W.S. Yang, J.H. Noh, N.J. Jeon, Y.C. Kim, S. Ryu, J. Seo, S.I. Seok, *Science*, 2015, **348**, 1234.
- T. Salim, S. Sun, Y. Abe, A. Krishna, A.C. Grimsdale, Y.M. Lam, *J. Mater. Chem. A*, 2015, **3**, 8943.
- M. Liu, M.B. Johnson, H.J. Snaith, *Nature*, 2013, **501**, 395.
- (a) H.-R. Xia, W.-T. Sun, L.-M. Peng, *Chem. Commun.*, 2015, **51**, 13787; (b) C. Muthu, S.R. Nagamma, V.C. Nair, *RSC Adv.*, 2014, **4**, 55908.
- Y. Jin, G. Chumanov, *Appl. Mater. Interfaces*, 2015, **7**, 12015.
- N. Yantara, D. Sabba, F. Yanan, J.M. Kadro, T. Moehl, P.P. Boix, S. Mhaisalkar, M. Grätzel, C. Grätzel, *Chem. Commun.*, 2015, **51**, 4603.
- P.J. Holliman, A. Connell, E.W. Jones, S. Ghosh, L. Furnell, R.J. Hobbs, *Mater. Res. Innov.*, 2016, **19**, 508.
- J. Burschka, N. Pellet, S.J. Moon, R. Humphry-Baker, P. Gao, M.K. Nazeeruddin, M. Grätzel, *Nature*, 2013, **499**, 316.
- S. Luo, W.A. Daoud, *J. Mater. Chem. A*, 2015, **3**, 8992.
- L.C. Schmidt, A. Pertega, S. Gonzalez-Carrero, O. Malinkiewicz, S. Agouram, G. M. Espallargas, H.J. Bolink, R.E. Galian, J. Perez-Prieto, *J. Am. Chem. Soc.*, 2014, **136**, 850.
- Y. Wu, A. Islam, X. Yang, C. Qin, J. Liu, K. Zhang, W. Peng, L. Han, *Energy Environ. Sci.*, 2014, **7**, 2934.
- M.J. Carnie, C. Charbonneau, M.L. Davies, J. Troughton, T.M. Watson, K. Wojciechowski, H. Snaith, D.A. Worsley, *Chem. Commun.*, 2013, **49**, 7893.
- Y. Deng, E. Peng, Y. Shao, Z. Xiao, Q. Dong, J. Huang, *Energy Environ. Sci.*, 2015, **8**, 1544.
- P.J. Holliman, D.K. Muslem, E.W. Jones, A. Connell, M.L. Davies, C. Charbonneau, M.J. Carnie, D.A. Worsley, *J. Mater. Chem. A*, 2014, **2**(29), 11134.
- J.M. Ball, M.M. Lee, A. Hey, H.J. Snaith, *Energy Environ. Sci.*, 2013, **6**, 1739.
- N. Espinosa, L. Serrano-Luján, A. Urbino, F.C. Krebs, *Solar Energy Mater. Solar Cells*, 2015, **137**, 303.
- Q. Chen, H. Zhou, Y. Fang, A.Z. Stieg, T.-B. Song, H.-H. Wang, X. Xu, Y. Liu, S. Lu, J. You, P. Sun, J. McKay, M.S. Goorsky, Y. Yang, *Nat. Commun.*, 2015, **6**, 7269.
- H.-S. Ko, J.-W. Lee, N.-G. Park, *J. Mater. Chem. A*, 2015, **3**, 8808.
- F. Deschler, M. Price, S. Pathak, L.E. Klüntberg, D.-D. Jarausch, R. Higler, S. Hüttner, T. Leitjens, S.D. Stranks, H.J. Snaith, M. Atatüre, R.T. Phillips, R.H. Friend, *J. Phys. Chem. Lett.*, 2014, **5**, 1421.
- M. De Bastiani, V. D'Innocenzo, S.D. Stranks, H.J. Snaith, A. Petrozza, *APL Mater.*, 2014, **2**, 081509.
- V. D'Innocenzo, G. Grancini, M.J.P. Alcocer, A.R.S. Kandada, S.D. Stranks, M.M. Lee, G. Lanzani, H.J. Snaith, A. Petrozza, *Nat. Commun.*, 2014, **5**, 3586.
- C.-Y. Chang, C.-Y. Chu, Y.-C. Huang, S.-Y. Chang, C.-A. Chen, C.-Y. Chao, W.-F. Su, *Appl. Mater. Interfaces*, 2015, **7**, 4955.
- N.-J. Jeon, J.-H. Noh, Y.-C. Kim, W.-S. Yang, S. Ryu, S.-I. Seok, *Nature Mat.*, 2014, **13**, 897.
- Y. Zhou, M. Yang, W. Wu, A.L. Vasiliev, K. Zhu, N.P. Padture, *J. Mater. Chem. A*, 2015, **3**, 8179.